Electromagnetic Scattering by Spherical Particles

Kirk A Fuller

April, 2024*

*Last updated July 11, 2024

Contents

1 Theory for Homogeneous Spheres **2**

1.1 The Vector Spherical Wave Functions . . . 3

1.2 The Response of a Sphere to Harmonic Plane Waves . . . 4

1.3 Cross Sections . . . 5

2 Theory for Concentrically Stratified Spheres **8**

2.1 Reflection and Transmission of an Outgoing Spherical Wave at a Concentric, Concave Spherical Boundary . . . 8

2.2 The Scattering Coefficients of a Concentrically Coated Sphere . . . 9

2.2.1 A test of the backscatter efficiency of a coated sphere . . . 10

3 Polarimetric Scattering **12**

4 Nonspherical Particles and the T Matrix **15**

5 Appendix **18**

5.1 FULMIE Routines . . . 18

5.1.1 The a_{np} Algorithm . . . 18

5.1.2 The Q_{abs} algorithm . . . 19

5.1.3 The τ_{mnp} algorithm . . . 20

5.2 FULKOT Routines . . . 21

5.2.1 Calculation of the cap ($\hat{}$) coefficients . . . 21

5.2.2 Calculation of the amplitude coefficients of the core . . . 23

5.2.3 Calculation of Spherical Bessel Functions for Large $\Im(\eta)$ . . . 23

5.2.4 Asymptotes for Downward Recursion . . . 25

1 Theory for Homogeneous Spheres

Understanding the interaction of a homogeneous sphere with an electromagnetic plane wave is to optical scattering and electromagnetic theory what the hydrogen atom problem is to spectroscopy and quantum mechanics. The study of each begins with a wave equation, expressed in spherical coordinates, and lays the groundwork for the study of more complicated problems. The wave equation for the former is derived from Maxwell's equations, and for the latter, from the Schroödinger equation for a potential proportional to $1/r$.

We begin with the free space Maxwell equations

$$\begin{aligned} \nabla \cdot \epsilon_0 \mathbf{E} &= 0 \\ \nabla \cdot \mu_\mathbf{0} \mathbf{H} &= 0 \\ \nabla \times \mathbf{E} &= -\frac{\partial \mu_0 \mathbf{H}}{\partial t} \\ \nabla \times \mathbf{H} &= \frac{\partial \epsilon_0 \mathbf{E}}{\partial t}. \end{aligned} \tag{1}$$

From these equations, it can be shown that

$$\nabla^2 \mathbf{E} - \epsilon_0 \mu_0 \frac{\partial^2 \mathbf{E}}{\partial t^2} = 0. \tag{2}$$

Noting that the expression for a vector wave traveling at speed v is

$$\nabla^2 \mathbf{E} - \frac{1}{v^2} \frac{\partial^2 \mathbf{E}}{\partial t^2} = 0, \tag{3}$$

it is seen that Maxwell's equations successfully predict the speed of light ($v_0 = 1/\sqrt{\epsilon_0 \mu_0}$).

For fields that are time-harmonic and of wavelength λ_0, Eq. 2 takes the form

$$\nabla^2 \mathbf{E} + k_0^2 \mathbf{E} = \mathbf{0}, \tag{4}$$

where $k_0 = 2\pi/\lambda_0$. The equation for $\mathbf{H}$ is identical. This is the vector Helmholtz equation. If the wave is propagating through a homogeneous, nonabsorbing medium then Eq. 4 takes the form

$$\nabla^2 \mathbf{E} + k_0^2 \left[\frac{\epsilon \mu}{\epsilon_0 \mu_0} \right] \mathbf{E} = \mathbf{0}.$$

The quantity in square brackets is the square of the ratio of the speed of light in vacuum to its speed in the medium, i.e. the square of the refractive index, n, of the medium.

When there is absorption, there is a migration of charge associated with atomic and molecular transitions which we understand to be a microscopic current. The current can be expressed by Ohm's law as $\sigma \mathbf{E}$, where σ is the wavelength-dependent conductivity of the medium. This current must be added to the displacement current ($\partial \epsilon \mathbf{E}/\partial t$), which then leads to

$$\nabla^2 \mathbf{E} + k_0^2 \left[\frac{\epsilon \mu}{\epsilon_0 \mu_0} + \frac{i\sigma}{\epsilon_0 \mu_0} \right] \mathbf{E} = \mathbf{0}.$$

Thus, we are naturally led to the concept of a complex refractive index $\mathsf{m} = \mathsf{n} + i\mathsf{k}$, where k is known as the absorptive index of the medium.

1.1 The Vector Spherical Wave Functions

In many areas of physical optics, problems are best solved in Cartesian coordinates, but in the case of scattering by a particle we are dealing with outgoing spherical waves. This means that we will need solutions to the vector Helmholtz equation in spherical coordinates.

$$\nabla^2 \mathbf{E}^{inc} + k^2 \mathbf{E}^{inc} = \mathbf{0}, \qquad \text{and} \qquad \nabla^2 \mathbf{E}^{sca} + k^2 \mathbf{E}^{sca} = \mathbf{0}, \tag{5}$$

In view of Eq. 4, the basis functions $\mathbf{M}$ used to mathematically represent the fields $\mathbf{E}$ and $\mathbf{H}$ must satisfy $\nabla^2\mathbf{M}+k^2\mathbf{M}=\mathbf{0}$. Since $\mathbf{M}$ must also satisfy $\nabla \cdot \mathbf{M} = \mathbf{0}$, the simplest choice for this function is $\mathbf{M} = \nabla \times \mathbf{v}\psi$. Substitution of this expression for $\mathbf{M}$ into Eq. (2), and manipulation of the resulting expressions with the use of identities from vector calculus leads one to the conclusion that it is sufficient that $\mathbf{M}$ satisfy Eq. (2) in spherical coordinates if $\mathbf{v} = \mathbf{r}$ and ψ satisfies the scalar wave equation $\nabla^2\psi + k^2\psi = 0$. While the above discussion is specific to spherical coordinates, and follows Stratton (1941, Chapter 7) and Bohren and Huffman (1983, Chapter 4), Morse and Feschbach (1953, Chapter 13) provide an elegant treatment for identifying $\mathbf{v}\psi$ in generalized curvilinear coordinates.

A second set of functions that are orthogonal to $\mathbf{M}$ and which likewise satisfy Eq. (2) are $\mathbf{N} = \nabla \times \mathbf{M}/k$. The scalar wave equation is separable in spherical coordinates and the separation constants are integers m and n. The solution to the scalar equation is a complete set of mutually orthogonal functions ψ_{mn}. A construction of these functions is given by Bohren and Huffman (1983, Chapter 4). The functions $\mathbf{M}$ and $\mathbf{N}$ thus comprise a complete set of mutually orthogonal functions, and therefore all functions satisfying Eq. (2) may be projected onto the $\mathbf{M}, \mathbf{N}$ basis. In order to streamline the notation, which becomes rather ornate as one proceeds to more complicated particle morphologies, we introduce the index $p = 1, 2$ for reference to the TM ($\mathbf{N}$), TE ($\mathbf{M}$) modes of the electric field.

Introducing the angle dependent functions τ_{mnp},

$$\tau_{mn1}(\cos\vartheta) = \frac{d}{d\vartheta} P_n^m(\cos\vartheta) \tag{6}$$

and

$$\tau_{mn2}(\cos\vartheta) = \frac{m}{\sin\vartheta} P_n^m(\cos\vartheta), \tag{7}$$

where P_n^m are associated Legendre functions, along with the position vector $\mathbf{r} = r\,\hat{\mathbf{r}}$ ($\hat{\mathbf{r}} = \mathbf{r}/|\mathbf{r}|$), the vector spherical wave functions (VSWF) may be written as

$$\begin{aligned} \mathbf{N}_{mnp}(k\mathbf{r}) \quad = \quad & e^{im\varphi}\left[(2-p)\frac{\zeta_n(kr)}{(kr)^2} n(n+1) P_n^m(\cos\vartheta)\,\hat{\mathbf{r}}\right. \\ & \left. + i^{p-1}\,\frac{\zeta_n^{[2-p]}(kr)}{kr}\tau_{mnp}(\cos\vartheta)\,\hat{\boldsymbol{\vartheta}} + i^p\,\frac{\zeta_n^{[2-p]}(kr)}{kr}\tau_{mn(3-p)}(\cos\vartheta)\,\hat{\boldsymbol{\varphi}}\right], \end{aligned} \tag{8}$$

where $\hat{\boldsymbol{\vartheta}}$ and $\hat{\boldsymbol{\varphi}}$ are unit vectors in the directions of the polar and azimuthal angles ϑ and φ, respectively. The $\zeta_n^{[0]} \equiv \zeta_n$ are Ricatti-Bessel functions, with prime derivatives denoted $\zeta_n^{[1]}$, which will be expressed in

terms of either spherical Hankel functions of the first kind as $\xi_n(kr) = kr\, h_n^{(1)}(kr)$ or as spherical Bessel functions $\psi_n(kr) = Rg\,\xi_n = kr\, j_n(kr)$. The reader is cautioned when referring to the literature that τ_{mn1} and τ_{mn2} are often written as τ_{mn} and π_{mn} (or $-\pi_{mn}$ and τ_{mn}, cf. Fuller, 1987; Kerker, 1969; Bruning and Lo, 1971). The VSWF are given in a more conventional form by Fuller (1994a).

1.2 The Response of a Sphere to Harmonic Plane Waves

The ability of a particle to scatter light depends upon its characteristic size s, the wavelength λ of the incident light, and its complex index of refraction $\mathsf{m}(\lambda)$ relative to that of the surrounding medium. (For now, the relative magnetic permeability is assumed to be 1.) Parameters of the form $k\mathsf{s}$ and $\mathsf{m}k\mathsf{s}$, $k = 2\pi/\lambda$, are typically used to describe the 'optical' dimensions of the scattering system. For a sphere, s is simply its radius, $r = a$.

To quantify the response of a sphere to a train of electromagnetic waves with planar surfaces of constant phase and unit amplitude it is best to interpret those waves into the 'native language' of the sphere, i.e., to expand the plane wave in VSWF:

$$\mathbf{E}^{inc} = \mathbf{E}_0 \exp\left[ik\,\mathbf{r}\cdot\mathbf{n}^{inc}\right] = \sum_{n=1}^{\infty}\sum_{m=-n}^{n}\sum_{p=1}^{2} q_{mnp} Rg\mathbf{N}_{mnp}, \tag{9}$$

where $\mathbf{n}^{inc}$ is the unit vector in the direction of incidence and Rg means that only the part of ζ that is regular at the origin, viz. ψ_n is used. Hansen (1935, 1937) was the first to formulate such an expansion, and the $\mathbf{N}_{mnp}$ are sometimes referred to as Hansen's functions.

The expansion for the scattered field may be written as

$$\mathbf{E}^{sca} = \sum_{m,n,p} q_{mnp} a_{np} \mathbf{N}_{mnp} = \sum_{m,n,p} a_{mnp} \mathbf{N}_{mnp}.$$

The expansion in Eq. (9) allows us to decompose the plane wave into spherical partial waves with amplitudes q_{mnp}. For practical purposes the expansion of $\mathbf{E}^{inc}$ can be truncated after enough partial waves are included to reproduce $\mathbf{E}_0 \exp\left[ik\,\mathbf{r}\cdot\mathbf{n}^{inc}\right]$ at the surface of the sphere with sufficient accuracy, thus allowing one to match boundary conditions and extract the coefficients of the scattered field. A frequently used estimate of the maximum order n_{max} required in the expansion is obtained from the criterion developed by Wiscombe (1980), i.e.,

$$n_{max} = \varrho + 4.05\varrho^{1/3} + 2, \qquad \varrho = ka \tag{10}$$

Adopting the notation $\psi_n(\varrho) = \varrho j_n(\varrho)$ and $\xi_n(\varrho) = \varrho h_n^{(1)}(\varrho)$, the coefficients a_{np} are found from the boundary conditions at the surface of the sphere to be

$$a_{n1} = -\frac{\mathsf{m}\psi_n'(\varrho)\,\psi_n(\eta) - \psi_n(\varrho)\,\psi_n'(\eta)}{\mathsf{m}\xi_n'(\varrho)\,\psi_n(\eta) - \xi_n(\varrho)\,\psi_n'(\eta)} \tag{11}$$

and

$$a_{n2} = -\frac{\mathsf{m}\psi_n(\varrho)\,\psi_n'(\eta) - \psi_n'(\varrho)\,\psi_n(\eta)}{\mathsf{m}\xi_n(\varrho)\,\psi_n'(\eta) - \xi_n'(\varrho)\,\psi_n(\eta)}, \tag{12}$$

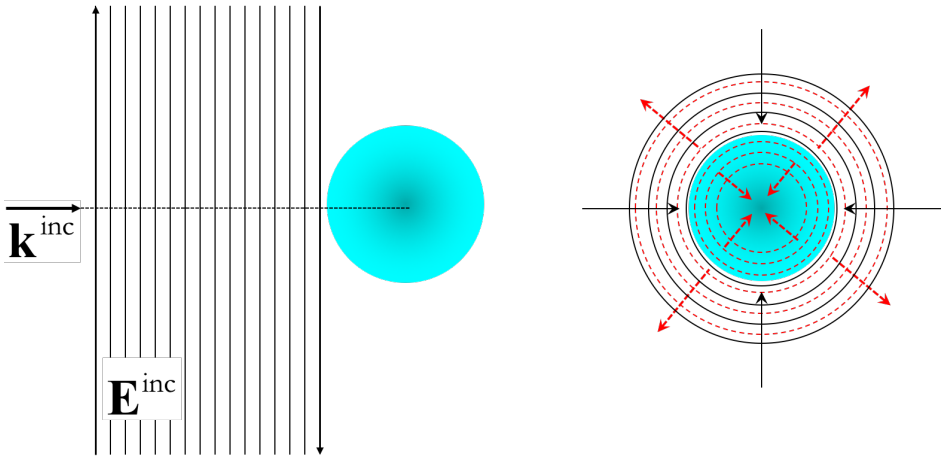

Figure 1: Projection of an incident plane wave onto the VSWF basis set. In other words, representing planar surfaces of constant phase as a superposition of spherical surfaces of constant phase. An infinite plane wave is depicted on the left. On the right, the black circles represent the spherical wave components of the incident field, while the red circles represent the scattered and internal fields produced by the interaction of the sphere with the incident field.

with $\eta = \mathsf{m}\varrho$. These coefficients are variously named after Lorenz, Mie and Debye, and we refer to them here as LM coefficients (most authors have written a_{n1} and a_{n2} as a_n and b_n, respectively). The a_{np} coefficients are complex amplitudes which quantify the response of the sphere to the nth partial wave in the plane wave decomposition. They are completely analogous to the Fresnel coefficients for a plane wave reflecting from a flat surface, and follow from the same simple algebra once the boundary conditions are imposed. The more difficult part of this process is finding the coefficients p_{mnp}, which is discussed in Stratton (1941, Chapter 7) and in Morse and Feschbach (1953, Chapter 13). (One commonly sees q_{mnp} written as p_{mn} and q_{mn} for $p = 1$ and 2, respectively.) For particles with spherical symmetry, the coordinate system can be chosen so that the incident field propagates parallel to the z axis of the body-centered coordinate frame, i.e., $\mathbf{n}^{inc} = \mathbf{e}_z$, and this will lead to important simplifications that allow us to write the scattered electric field in the standard notation:

$$\mathbf{E}^{sca} = \sum_{n=1}^{\infty} i^n \frac{2n+1}{n(n+1)} \left[i a_n \mathbf{N}^{(3)}_{e1n} - b_n \mathbf{M}^{(3)}_{o1n} \right] \text{(Bohren and Huffman, 1983)} \tag{13}$$

$$= \sum_{n=1}^{\infty} \sum_{p=1}^{2} i^p \cos(\varphi - p\pi/2) \left[a_{1np} \mathbf{N}_{1np} \right] \text{(this work)}. \tag{14}$$

1.3 Cross Sections

For an unpolarized beam of unit intensity incident along the z axis, the scattered power into the solid angle $d\Omega$ is proportional to the S_{11} element of the sphere's phase matrix, otherwise known as the differential scattering cross section $\frac{dC_{sca}}{d\Omega}$. The scattering cross section may be written as

$$C_{sca} = \int_{\Omega} \frac{\text{Energy scattered/unit time/unit solid angle}}{\text{Incident energy flux (energy/unit area/unit time)}} \, d\Omega = \int_{4\pi} \frac{dC_{sca}}{d\Omega} \, d\Omega. \tag{15}$$

The phase function is defined to be

$$a_1(\vartheta) = \frac{4\pi}{C_{sca}} \frac{dC_{sca}}{d\Omega} \tag{16}$$

and the scattered intensity at a distance r from the particle is then simply

$$I^{sca} = \frac{C_{sca}\, a_1(\vartheta)\, I^{inc}}{4\pi r^2}\,. \tag{17}$$

The free-space Maxwell's equations for time-harmonic fields allow us to write the scattered magnetic field as $\mathbf{H}^{sca} = -i\nabla \times \mathbf{E}^{sca}/\omega\mu_0$, where μ_0 is the permeability of free space and ω is the free-space angular frequency, and the total scattering cross section, C_{sca}, can be found from an integral of the time-averaged Poynting flux of scattered radiant energy $\mathbf{E}^{sca} \times (\mathbf{H}^{sca})^*$ over all directions (ϑ, φ) :

$$C_{sca} = \frac{1}{\left|\mathbf{E}^{inc} \times (\mathbf{H}^{inc})^*\right|} \frac{1}{2} Re \int_0^{\pi} \int_0^{2\pi} \mathbf{E}^{sca} \times (\mathbf{H}^{sca})^* \cdot \mathbf{n}^{sca}\; r^2 \sin\vartheta \, d\vartheta \, d\varphi \tag{18}$$

where $\mathbf{E}^{inc} \times \left(\mathbf{H}^{inc}\right)^*$ is the Poynting flux of the incident field, and time-averaging over an interval that is much longer than the period of the stimulating radiation is accomplished with the complex conjugation ($*$) of $\mathbf{H}$ (Stratton, 1941, page 135). By integrating Eq. (18) over an imaginary spherical surface that is concentric with the scatterer, it can be shown that the scattering cross section of a sphere is

$$C_{sca} = \frac{2\pi}{k^2} \sum_{n=1}^{\infty} (2n+1)(|a_n|^2 + |b_n|^2) \tag{19}$$

$$= \frac{2\pi}{k^2} \sum_{n=1}^{\infty} \sum_{p=1}^{2} (2n+1)|a_{np}|^2. \tag{20}$$

The extinction cross section may be found from the optical theorem, vis.,

$$C_{ext} = \frac{2\pi}{k} \Im \left[S_{11}(0) + S_{22}(0)\right] \tag{21}$$

$$= \frac{2\pi}{k^2} \sum_{n=1}^{\infty} \sum_{p=1}^{2} (2n+1) \Re(a_{np}). \tag{22}$$

Conservation of energy then provides the absorption cross section $C_{abs} = C_{ext} - C_{sca}$, and the single scattering albedo $\varpi = C_{sca}/C_{ext}$. An expansion for the absorption cross section can be obtained by integrating the radial component of the Poynting vector for the internal field, evaluated at the surface of the sphere, *viz.*

$$C_{abs} = \frac{a^2}{\left|\mathbf{E}^{inc} \times (\mathbf{H}^{inc})^*\right|} \frac{1}{2} Re \int_0^{\pi} \int_0^{2\pi} \mathbf{E}^{tra} \times \left(\mathbf{H}^{tra}\right)^* \cdot (-\mathbf{n}^{sca})\; \sin\vartheta \, d\vartheta \, d\varphi. \tag{23}$$

The same expansion also follows from substitution of Eqs. (22) and (20) into $C_{ext} - C_{sca}$ (Kattawar and Eisner, 1970). The expansion for C_{abs} is

$$C_{abs} = \frac{2\pi}{|\mathsf{m}|^2 k^2} \sum_{n=1}^{\infty} (2n+1)\, \Re\; i\psi'_n(\eta)\, \psi_n^*(\eta) \left(\mathsf{m}\, |c_{n1}|^2 + \mathsf{m}^*\, |c_{n2}|^2\right), \tag{24}$$

where c_{np} are the expansion coefficients for the internal fields and can be written in terms of the LM coefficients as

$$c_{n1} = \frac{i\mathsf{m} a_{n1}}{\mathsf{m}\psi'_n(\rho)\, \psi_n(\eta) - \psi_n(\rho)\, \psi'_n(\eta)} \tag{25}$$

and

$$c_{n2} = \frac{i\mathsf{m}a_{n2}}{\mathsf{m}\psi_n(\rho)\,\psi'_n(\eta) - \psi'_n(\rho)\,\psi_n(\eta)}. \tag{26}$$

It is to be noted that c_{n1} and c_{n2} are interchanged in the notation of others (cf. Bohren and Huffman, 1983, p. 100; Mackowski, 1991). Care should also be taken with regard to sign: Bohren and Huffman define their coefficients to be of opposite sign to those used here.

One other quantity of great importance is the average cosine of the scattering angle—the asymmetry parameter. It is expressed in terms of the partial wave coefficients as

$$\langle\cos(\vartheta)\rangle = \frac{4\pi}{k^2\,C_{\mathrm{sca}}}\left\{\sum_{n=1}^{\infty}\frac{n(n+2)}{n+1}\left(a_{n1}\,a^*_{(n+1)1} + a_{n2}\,a^*_{(n+1)2}\right) + \sum_{n=1}^{\infty}\frac{2n+1}{n(n+1)}\Re\left(a_{n1}\,a^*_{n2}\right)\right\}. \tag{27}$$

2 Theory for Concentrically Stratified Spheres

The next level of complexity is the case of scattering and absorption by a concentrically stratified sphere. The solution parallels that for a homogeneous sphere, but with the interaction between the core and shell taken into account.

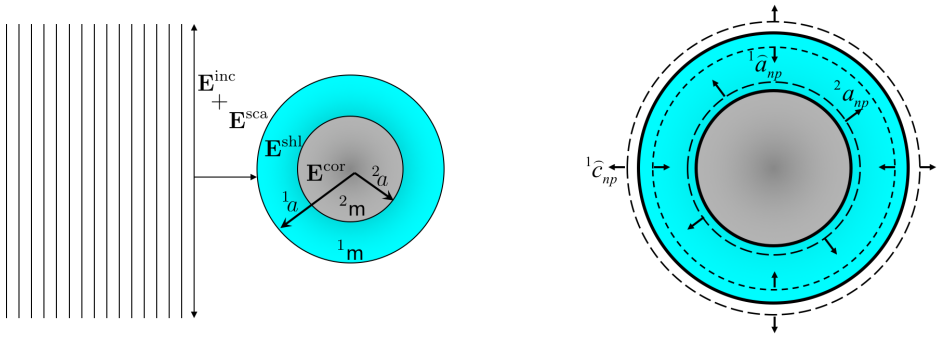

Figure 2: The projection of planar surfaces of constant phase onto the VSWF basis for a concentrically stratified sphere leads to a second set of expansion coefficients that arise from interactions between concentric concave and convex spherical surfaces. Here, $\hat{a}_n$ and $\hat{c}_n$ are, respectively, the coefficients for reflection and transmission of an out-going spherical wave at a concave spherical surface.

2.1 Reflection and Transmission of an Outgoing Spherical Wave at a Concentric, Concave Spherical Boundary

Consider now the case of an *outgoing* electric partial wave, represented by $\mathbf{E}_{mn} = \mathbf{N}_{mn} + \mathbf{M}_{mn}$, that crosses a spherical dielectric discontinuity of radius r_1 centered about the coordinate system to which the VSWF are referenced. Let the refractive index of the interior region be m_1 and that of the exterior be unity. The outgoing field will be partially reflected and partially transmitted at the interface. The tangential components of the exterior (transmitted) partial field must match the sum of the interior (incident + reflected) partial fields at the boundary and we may therefore write

$$\left[{}^1\hat{c}_n\mathbf{N}_{mn1} + {}^1\hat{d}_n\mathbf{N}_{mn2}\right]_{\vartheta,\varphi} = \left[{}^1\hat{a}_n Rg\mathbf{N}_{mn1} + {}^1\hat{b}_n Rg\mathbf{N}_{mn2} + \mathbf{N}_{mn1} + \mathbf{N}_{mn2}\right]_{\vartheta,\varphi}. \tag{28}$$

Because of the orthogonality properties of the VSWF, there is no coupling of mn to $m'n'$ normal modes (nor is there coupling between TE and TM modes) at the boundary. Thus the angular dependence of the ϑ and φ components of the partial fields cancel algebraically in Eq. (28). Because of the different refractive indices on either side of the boundary, the radial functions do not cancel and we have

$$\mathsf{m}_1\,{}^1\hat{c}_n\xi_n'(\rho_1) = \xi_n'(\eta_1) + {}^1\hat{a}_n\psi_n'(\eta_1), \tag{29}$$

where $\rho_1 = kr_1$ and $\eta_1 = \mathsf{m}_1\rho_1$. From the magnetic counterpart of Eq. (29) we obtain

$${}^1\hat{c}_n\xi_n(\rho_1) = \xi_n(\eta_1) + {}^1\hat{a}_n\psi_n(\eta_1), \tag{30}$$

thus

$$ {}^1\hat{c}_n = \frac{\psi_n(\eta_1)\xi'_n(\eta_1) - \xi_n(\eta_1)\psi'_n(\eta_1)}{\mathsf{m}^1\xi'_n(\rho_1)\psi_n(\eta_1) - \xi_n(\rho_1)\psi'_n(\eta_1)}. \tag{31} $$

Precisely the same arguments produce the expressions

$$ {}^1\hat{a}_n = -\frac{\mathsf{m}_1\xi'_n(\rho_1)\xi_n(\eta_1) - \xi_n(\rho_1)\xi'_n(\eta_1)}{\mathsf{m}_1\xi'_n(\rho_1)\psi_n(\eta_1) - \xi_n(\rho_1)\psi'_n(\eta_1)}, \tag{32} $$

$$ {}^1\hat{d}_n = -\frac{\psi_n(\eta_1)\xi'_n(\eta_1) - \xi_n(\eta_1)\psi'_n(\eta_1)}{\mathsf{m}^1\xi_n(\rho_1)\psi'_n(\eta_1) - \xi'_n(\rho_1)\psi_n(\eta_1)}, \tag{33} $$

$$ {}^1\hat{b}_n = -\frac{\mathsf{m}_1\xi_n(\rho_1)\xi'_n(\eta_1) - \xi'_n(\rho_1)\xi_n(\eta_1)}{\mathsf{m}_1\xi_n(\rho_1)\psi'_n(\eta_1) - \xi'_n(\rho_1)\psi_n(\eta_1)}, \tag{34} $$

and for incoming spherical waves, the standard LM coefficients are given as ${}^1a_{n1} \equiv a_n$, ${}^1a_{n2} \equiv b_n$, ${}^1c_{n1} \equiv c_n$, and ${}^1c_{n2} \equiv d_n$.

For incoming spherical waves, the LM coefficients of order n for the scattered and internal partial fields are the spherical wave analogues to the Fresnel coefficients for reflection and refraction of a plane wave at a planar boundary. With the derivation of the '^' (cap) coefficients (Fuller, 1993a,b; Mackowski and Jones, 1995), the analogy can now be extended to the case of *outgoing* spherical waves reflected and transmitted by *concave* spherical surfaces. Application of these concepts leads to an elegant solution of the standard concentrically stratified sphere problem. This solution is summarized in the next subsection.

2.2 The Scattering Coefficients of a Concentrically Coated Sphere

The following treatment is an alternative to the original derivation by Aden and Kerker (1951). Perhaps the simplest coefficients for reflection and transmission by multilayered structures are those based on coefficients for a thin film, where $r_{\ell p}$, $\hat{r}_{\ell p}$, $t_{\ell p}$, and $\hat{t}_{\ell p}$ represent the Fresnel coefficients for reflection and transmission at the surfaces indicated for orthogonal polarizations p. In this case we may express the amplitude of the electric field reflected by the film as

$$ E_p^{ref} = rE_p^{inc}, \tag{35} $$

$$ E_p^{ref} = E_p^{inc}\left(r_{1p} + t_{1p}\, r_{2p}\, \hat{t}_{1p} \sum_{k=0}^{\infty} [r_{2p}\, \hat{r}_{1p}]^k\right) \tag{36} $$

$$ = E_p^{inc}\left(r_{1p} + \frac{t_{1p}\, r_{2p}\, \hat{t}_{1p}}{1 - [r_{2p}\, \hat{r}_{1p}]}\right). \tag{37} $$

Posing the problem of electromagnetic scattering by concentrically coated spheres as one of multiple reflection of spherical partial waves, as illustrated in Fig. 3, one is led to a surprisingly simple solution (Fuller, 1993a,b): The scattering coefficients can be expressed as

$$ {}^1a_{1np} = q_{1np}\left({}^1a_{np} + {}^1c_{np}\, {}^2a_{np}\, {}^1\hat{c}_{np} \sum_{k=0}^{\infty} \left[{}^2a_{np}\, {}^1\hat{a}_{np}\right]^k\right) \tag{38} $$

$$ = q_{1np}\left({}^1a_{np} + \frac{{}^1c_{np}\, {}^2a_{np}\, {}^1\hat{c}_{np}}{1 - [{}^2a_{np}\, {}^1\hat{a}_{np}]}\right), \tag{39} $$

and the scattered field may be written as

$$\mathbf{E}^{sca} = \sum_{n,p} i^p \cos(\varphi - p\pi/2) \left[{}^1a_{1np}\mathbf{N}_{1np} \right] \longrightarrow \sum_{n=1}^{\infty} i^n \frac{2n+1}{n(n+1)} \left(i\, a_n^T \mathbf{N}_{e1n}^{(3)} - b_n^T \mathbf{M}_{o1n}^{(3)} \right). \tag{40}$$

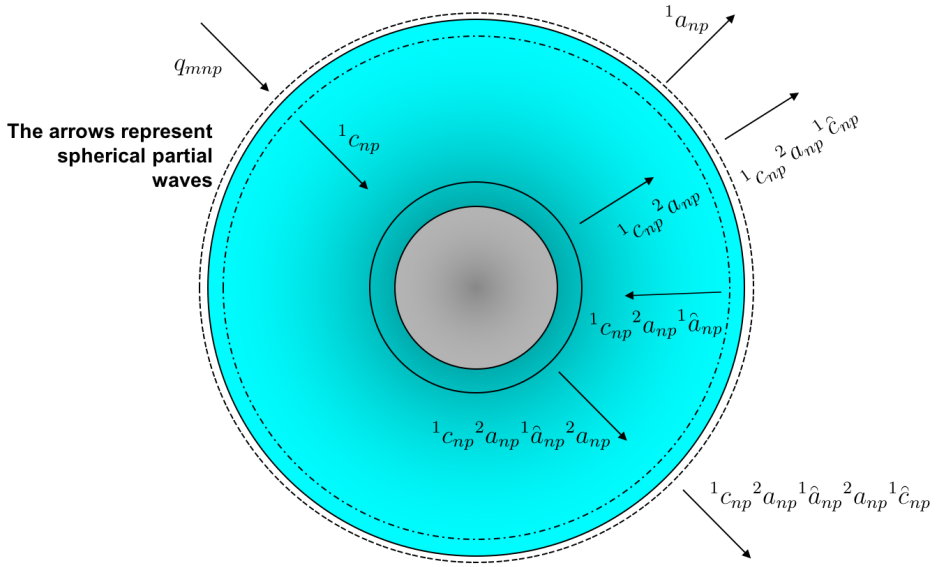

$$a_{np} = {}^1a_{np} + {}^1c_{np}\,{}^2a_{np}\,{}^1\hat{c}_{np} \sum_{j=0}^{\infty} \left[{}^2a_{np}\,{}^1\hat{a}_{np} \right]^j$$

Figure 3: Evolution of fields by multiple reflection of partial waves.

Because the structure of Eq. (40) is the same as that of Eq. (13), all of the radiometric properties discussed in the previous section will be of the same form, but with a_n^T and b_n^T replacing a_n and b_n. That structure also suggests features, perhaps observed by Essien *et al.* (1993), that cast the stratified sphere as a concave-convex spherical resonator. In addition to better physical insight, Eq. (39) also allows implementation of a coated sphere algorithm with the addition of only a few lines of code to an existing LM program. This algorithm also avoids the problems of numerical instability encountered by Bohren and Huffman (1983, p. 484). Another numerically stable algorithm is provided by Toon and Ackerman (1981).

Recursive algorithms for multilayered spheres have been developed by Bhandari (1985) and by Mackowski *et al.* (1990), and the treatment in this section also readily lends itself to a recursive treatment that parallels that for multilayered films. An example (out of many) of the use of multilayered spheres to model the optical properties of droplets with radially varying refractive index is provided by Massoli (1998).

2.2.1 A test of the backscatter efficiency of a coated sphere

To test the Q_b calculation we follow Bohren and Huffman's example for the homogeneous sphere wherein they show that $Q_b \longrightarrow R(0°)$. The reflectance at normal incidence for a film of thickness d and refractive

index m_f on a semi infinite substrate with refractive index m_S can be found from Eq.(37), where

$$r_{1p} = \frac{\mathsf{m}_f - 1}{\mathsf{m}_f + 1} \tag{41}$$

$$t_{1p} = \frac{2}{\mathsf{m}_f + 1} \tag{42}$$

$$r_{2p} = \frac{\mathsf{m}_S - \mathsf{m}_f}{\mathsf{m}_S + \mathsf{m}_f} \exp\left(i\,\mathsf{m}_f\,k_0 d\right) \tag{43}$$

$$\hat{r}_{1p} = -\frac{\mathsf{m}_f - 1}{\mathsf{m}_f + 1} \exp\left(i\,\mathsf{m}_f\,k_0 d\right) \tag{44}$$

$$\hat{t}_{1p} = \frac{2\,\mathsf{m}_f}{\mathsf{m}_f + 1} \exp\left(i\,\mathsf{m}_f\,k_0 d\right) \tag{45}$$

The resulting $r_{2p} \exp\left(i\,\mathsf{m}_f\,k_0 d\right)$ is a quantity that tells the first illuminated surface where the returning wave has been, and what it saw that made it come back. In fact, with these definitions, we rewrite Eq. (37) as

$$r_p = r_{1p} + \frac{t_{1p} r_{2p} \hat{t}_{1p}}{1 - [r_{2p}\,\hat{r}_{1p}]} E_p^{inc}, \tag{46}$$

and then as long as significant 'retroreflection' is avoided,

$$Q_{180^\circ} = |r_p|^2 \tag{47}$$

In Fig. 4, calculations of the backscatter efficiency for coated spheres of varying shell thickness are compared to the normal-incidence reflectance of a thin film, also of varying thickness. This comparison follows the lead of Bohren and Huffman, wherein the backscatter efficiency of an absorbing homogeneous sphere is related to the normal incidence reflectance of a thick slab of the same material. It is seen that backscatter efficiencies and reflectance are virtually identical when the core is able to absorb enough light to suppress a contribution to backscattering by internal reflections.

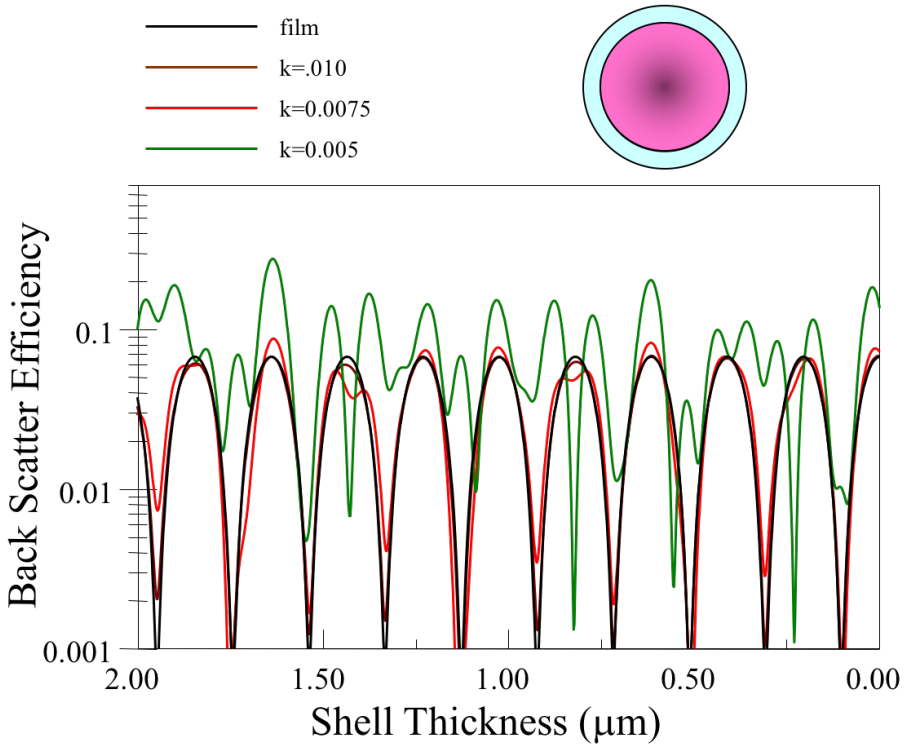

Figure 4: The backscatter efficiency of a coated sphere for different values of the imaginary part of the refractive index of the core. The real part of the refractive index of the core is 1.7, and the imaginary part takes on the values 0.01 (brown), 0.0075 (red), and 0.0050 (green). The normal incidence reflectance of a thin film is drawn in black.

3 Polarimetric Scattering

The incident and scattered electric fields are expressed here as expansions in vector spherical wave functions $\mathbf{N}_{mnp}$. Both $\mathbf{E}^{inc}$ and $\mathbf{E}^{sca}$ in the far field are transverse waves, each with two orthogonal components (polarizations). Information content comes in the form of the amplitudes and relative phase of the orthogonal components of those fields. It is important to note that for spheres and spheroids, the expansion of $\mathbf{E}^{sca}$ in terms of vector spherical wave functions is exact.

As a practical matter, only radiances can be measured. The Mueller matrix, denoted here as $\mathbf{F}$, provides the nexus between a set of radiance measurements (comprising the Stokes vector $\mathbf{I} = [I, Q, U, V]^T$) and the information carried in the fields themselves. For the case of ensembles of particles possessing sufficient symmetry, such as spheres and randomly oriented spheroids, the Mueller matrix is block diagonal and the scattered Stokes vector $\mathbf{I}_S$ in the scattering plane is found in terms of the Stokes vector $\mathbf{I}_0$ of the incident beam as $\mathbf{I}_S = \mathbf{F}\,\mathbf{I}_0$.

The elements of $\mathbf{F}$ are derived from the amplitudes and relative phases of the fields. If oriented, nonspherical particles are involved or when there is a need for rotational transformations of incident and scattered coordinate frames (as is usually the case), then the off-diagonal blocks are usually different from zero. An ex-

cellent discussion of the role of the Mueller (or phase) matrix in scattering theory is contained in Mishchenko et al. (2002).

The Mueller matrix contains the information on amplitudes and relative phases because it is derived from the 2×2 amplitude matrix $\mathbf{S}$. This matrix operates on the incident field to provide the scattered far-field in terms of components that are parallel ($\hat{\boldsymbol{\vartheta}}^{sca}$) and perpendicular ($\hat{\boldsymbol{\varphi}}^{sca}$) to the scattering plane. In general:

$$\begin{pmatrix} E_{\vartheta}^{sca} \\ E_{\varphi}^{sca} \end{pmatrix} = \begin{pmatrix} S_2 & S_3 \\ S_4 & S_1 \end{pmatrix} \begin{pmatrix} E_{\vartheta}^{inc} \\ E_{\varphi}^{inc} \end{pmatrix},$$

i.e.,

$$\mathbf{E}^{sca} = \mathbf{S}(\vartheta^{sca})\,\mathbf{E}^{inc}.$$

The amplitude matrix for spherical particles can be expressed as

$$\mathbf{S}\left(\vartheta^{sca}\right) = \frac{i}{k}\sum_{n}\frac{2n+1}{n(n+1)}\begin{pmatrix} a_{n1}\tau_{n1}\left(\vartheta^{sca}\right) + a_{n2}\tau_{n2}\left(\vartheta^{sca}\right) & 0 \\ 0 & a_{n1}\tau_{n2}\left(\vartheta^{sca}\right) + a_{n2}\tau_{n1}\left(\vartheta^{sca}\right) \end{pmatrix}. \tag{48}$$

Typically, the meridional plane of the incident beam, the scattering plane of the particle, and the meridional plane of the observer do not coincide. This situation is described by Figs. 5 and 6.

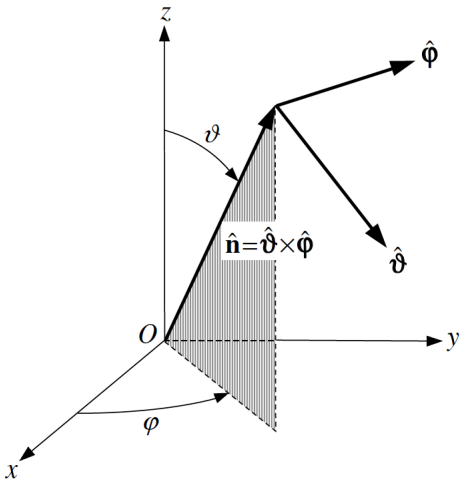

Figure 5: Incident plane.

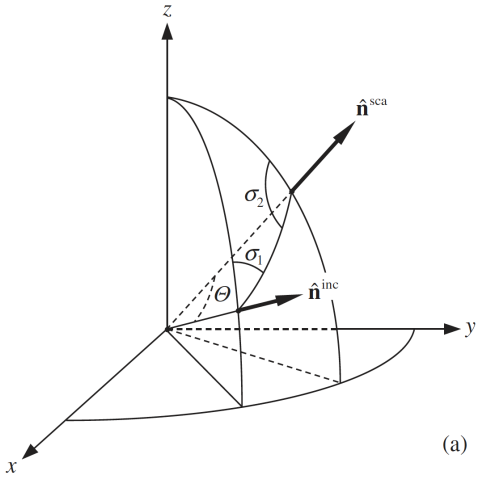

Figure 6: Scattering plane as related to the incident and emergent meridional planes. Here, Θ is the angle ϑ^{sca} in Eq. (48).

Because we are dealing with radiances, products of sines and cosines of the rotation angles for the field components are involved, and so the Mueller matrix elements involve double angles, and not simply the angles of rotation, for which the $\mathbf{S}$ matrix is

$$\mathbf{S}(\sigma) = \begin{pmatrix} \cos\sigma & \sin\sigma \\ -\sin\sigma & \cos\sigma \end{pmatrix}.$$

The Mueller matrix for a rotation through an angle σ is

$$\mathbf{L}(\sigma) = \begin{bmatrix} 1 & 0 & 0 & 0 \\ 0 & \cos 2\sigma & \sin 2\sigma & 0 \\ 0 & -\sin 2\sigma & \cos 2\sigma & 0 \\ 0 & 0 & 0 & 1 \end{bmatrix}. \tag{49}$$

The Mueller matrix for spherically symmetric particles and for many cases involving randomly oriented, arbitrarily shaped particles, takes the block diagonal form

$$\mathbf{F}(\Theta) = \begin{bmatrix} a_1(\vartheta) & b_1(\vartheta) & 0 & 0 \\ b_1(\vartheta) & a_2(\vartheta) & 0 & 0 \\ 0 & 0 & a_3(\vartheta) & b_2(\vartheta) \\ 0 & 0 & -b_2(\vartheta) & a_4(\vartheta) \end{bmatrix}.$$

Two rotations are required to determine the signal received by the observer: the first accounts for the field components in the incident meridional plane being projected onto directions parallel and perpendicular to the scattering plane, the second then relates the field components relative to the scattering plane to those of the meridional plane of the observer. So

$$\mathbf{I}_S = \mathbf{L}(-\sigma_2)\mathbf{F}(\vartheta^{sca})\mathbf{L}(\pi - \sigma_1)\,\mathbf{I}_0.$$

4 Nonspherical Particles and the T Matrix

In many important cases, the compostion of the atmospheric aerosol includes nonspherical particles such as dust or soot, examples of which are shown in Fig. 7. Extension of scattering theory to nonspherical particles is something of a variation on the theme for the treatment of spherical particles: we begin with an expansion for the incident field, apply boundary conditions, and produce a set of coefficients for the scattered fields.

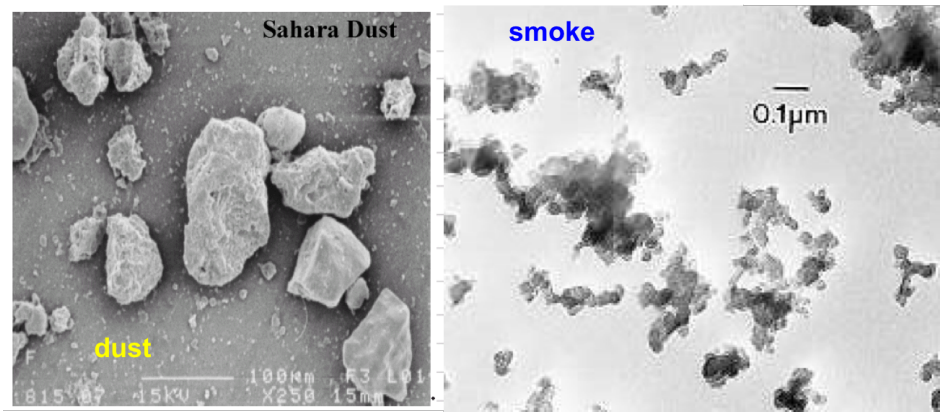

Figure 7: Typical examples of two major classes of nonspherical particles. On the left, mineral dust grains. On the right, smoke agglomerates.

Symbolically,

$$\mathbf{E}^{inc} = \sum_{n=1}^{\infty}\sum_{m=-n}^{n}\sum_{p=1}^{2} q_{mnp}\, Rg\mathbf{N}_{mnp} \quad \Rightarrow \quad \mathbf{E}^{sca} = \sum_{n=1}^{\infty}\sum_{m=-n}^{n}\sum_{p=1}^{2} q_{mnp}\, a_{mnp}\, \mathbf{N}_{mnp}, \tag{50}$$

where

$$\mathbf{E}^{sca} = \sum_{p=1}^{2}\sum_{n=1}^{\infty}\sum_{m=-n}^{n} a_{mnp}\mathbf{N}_{np} \tag{51}$$

$$a_{mnp} = -k_1(-1)^m \oint_S dS\Big\{\omega\mu\big[\hat{\mathbf{n}}\times\mathbf{H}_+(r)\big]\cdot Rg\mathbf{N}_{-mnp} - ik_1\big[\hat{\mathbf{n}}\times\mathbf{E}_+(r)\big]\cdot Rg\mathbf{N}_{-mn(3-p)}\Big\}. \tag{52}$$

This procedure can be written as

$$a_{mn1} = \sum_{\mu\nu}\big[T^{11}_{mn\mu\nu}\, q_{\mu\nu 1} + T^{12}_{mn\mu\nu}\, q_{\mu\nu 2}\big] \tag{53}$$

$$a_{mn2} = \sum_{\mu\nu}\big[T^{21}_{mn\mu\nu}\, q_{\mu\nu 1} + T^{22}_{mn\mu\nu}\, q_{\mu\nu 2}\big], \tag{54}$$

which can be cast in the form of a matrix operation

$$\begin{bmatrix}\mathbf{a}_1\\ \mathbf{a}_2\end{bmatrix} = \underbrace{\begin{bmatrix}\mathbf{T}^{11} & \mathbf{T}^{12}\\ \mathbf{T}^{21} & \mathbf{T}^{22}\end{bmatrix}}_{\text{Transition matrix}} \begin{bmatrix}\mathbf{q}_1\\ \mathbf{q}_2\end{bmatrix}, \tag{55}$$

or simply

$$\mathbf{a} = \mathbf{T}\mathbf{q}. \tag{56}$$

The challenge is to find the matrix elements. This involves large numbers of numerical integrations (generally) and inversion of large matrices, as outlined below. We begin with the T-matrix expressed as

$$\mathsf{T} = -\big(\mathrm{Rg}\,\mathsf{Q}\big)\mathsf{Q}^{-1}. \tag{57}$$

The elements of Q are given by

$$Q^{11}_{mn\mu\nu} = -ik_1k_2J^{21}_{mn\mu\nu} - ik_1^2J^{12}_{mn\mu\nu} \tag{58}$$

$$Q^{12}_{mn\mu\nu} = -ik_1k_2J^{11}_{mn\mu\nu} - ik_1^2J^{22}_{mn\mu\nu} \tag{59}$$

$$Q^{21}_{mn\mu\nu} = -ik_1k_2J^{22}_{mn\mu\nu} - ik_1^2J^{11}_{mn\mu\nu} \tag{60}$$

$$Q^{22}_{mn\mu\nu} = -ik_1k_2J^{12}_{mn\mu\nu} - ik_1^2J^{21}_{mn\mu\nu}, \tag{61}$$

where

$$\begin{bmatrix} J^{11}_{mn\mu\nu} \\ J^{12}_{mn\mu\nu} \\ J^{21}_{mn\mu\nu} \\ J^{22}_{mn\mu\nu} \end{bmatrix} = (-1)^m \oint_S dS\hat{\mathbf{n}}\cdot \begin{bmatrix} Rg\mathbf{N}_{\mu\nu 2}(k_2\mathbf{r})\times\mathbf{N}_{-mn2}(k_1\mathbf{r}) \\ Rg\mathbf{N}_{\mu\nu 2}(k_2\mathbf{r})\times\mathbf{N}_{-mn1}(k_1\mathbf{r}) \\ Rg\mathbf{N}_{\mu\nu 1}(k_2\mathbf{r})\times\mathbf{N}_{-mn2}(k_1\mathbf{r}) \\ Rg\mathbf{N}_{\mu\nu 1}(k_2\mathbf{r})\times\mathbf{N}_{-mn1}(k_1\mathbf{r}) \end{bmatrix}, \qquad \text{NDGS} \tag{62}$$

and

$$dS\hat{\mathbf{n}} = \left[\frac{\partial\mathbf{r}}{\partial\theta}\times\frac{\partial\mathbf{r}}{\partial\phi}\right]d\theta d\phi \tag{63}$$

$$= \left[r^2\,\sin\theta\,\hat{\mathbf{r}} - r\sin\theta\,\frac{\partial r}{\partial\theta}\hat{\boldsymbol{\theta}} - r\frac{\partial r}{\partial\phi}\hat{\boldsymbol{\phi}}\right]d\theta d\phi. \tag{64}$$

The integrations are carried out using Gausian quadratures.

For rotationally symmetric particles having a plane of mirror symmetry bisecting that rotation axis, the Mueller matrix for a large ensemble of randomly oriented grains takes the form

$$\mathsf{F}(\vartheta) = \begin{bmatrix} a_1(\vartheta) & b_1(\vartheta) & 0 & 0 \\ b_1(\vartheta) & a_2(\vartheta) & 0 & 0 \\ 0 & 0 & a_3(\vartheta) & b_2(\vartheta) \\ 0 & 0 & -b_2(\vartheta) & a_4(\vartheta) \end{bmatrix}. \tag{65}$$

Importantly, the matrix elements may be expressed as an expansion in terms of Wigner functions

$$d^n_{\ell m}(\vartheta) = \sqrt{(n+m)!(n-m)!(n+\ell)!(n-\ell)!}\ \sum_k (-1)^k \frac{(\cos\tfrac{1}{2}\vartheta)^{2n-2k+m-\ell}(\sin\tfrac{1}{2}\vartheta)^{2k-m+\ell}}{k!(n+m-k)!(n-\ell-k)!)(\ell-m+k)!} \tag{66}$$

as

$$a_1(\vartheta) = \sum_{n=0}^{n_{max}} \alpha_1^n \, d_{00}^n(\vartheta) \tag{67}$$

$$a_2(\vartheta) + a_3(\vartheta) = \sum_{n=2}^{n_{max}} (\alpha_2^n + \alpha_3^n) \, d_{22}^n(\vartheta) \tag{68}$$

$$a_2(\vartheta) - a_3(\vartheta) = \sum_{n=2}^{n_{max}} (\alpha_2^n - \alpha_3^n) \, d_{2,-2}^n(\vartheta) \tag{69}$$

$$a_4(\vartheta) = \sum_{n=0}^{n_{max}} \alpha_4^n \, d_{00}^n(\vartheta) \tag{70}$$

$$b_1(\vartheta) = -\sum_{n=2}^{n_{max}} \beta_1^n \, d_{02}^n(\vartheta) \tag{71}$$

$$b_2(\vartheta) = -\sum_{n=2}^{n_{max}} \beta_2^n \, d_{02}^n(\vartheta). \tag{72}$$

Because of the factorials and integer exponentials in Eq. 66, simple recursion relations exist for their rapid generation. Also for the special cases of $\ell = m = 0$ and $\ell = 0$, the Wigner functions reduce to the more familiar Legendre polynomials and associated Legendre functions,

$$P_n(\cos\vartheta) = \; d_{00}^n(\vartheta)$$

and

$$P_n^m(\cos\vartheta) = \sqrt{\frac{(n+m)!}{(n-m)!}} \; d_{0m}^n(\vartheta)$$

respectively.

Because the Wigner coefficients constitute a complete set of orthogonal functions, the α and β coefficients can be found from integrals of the form

$$\chi_j^n = (n + 1/2) \int_0^\pi f_{\ell m}^n(\vartheta) \sin\vartheta \, d\vartheta, \tag{73}$$

where the χ_j^n represent any of the coefficients in the expansions, and $f_{\ell m}^n(\vartheta)$ represents a product of any of the quantities on the left-hand side of Eqs. 67-72 with the appropriate $d_{\ell m}^n(\vartheta)$ functions.

For direct backscatter,

$$\mathbf{F}(\pi) = \begin{bmatrix} a_1(\pi) & 0 & 0 & 0 \\ 0 & a_2(\pi) & 0 & 0 \\ 0 & 0 & -a_2(\pi) & 0 \\ 0 & 0 & 0 & a_1(\pi) - 2a_2(\pi) \end{bmatrix}, \tag{74}$$

Handetal **??**

5 Appendix

5.1 FULMIE Routines

Much work has been done on the numerical procedures needed to generate reliable models for microsphere optics. The algorithm for the Lorenz-Mie coefficients used in FULMIE is that of Wang and van de Hulst (Appl. Opt., 1991). The angle-dependent functions used to calculate the scattered fields are calculated in TAUMNP, and are based on recursion relations provided by Tsang et al. (1985) and by Fuller (1987).

5.1.1 The a_{np} Algorithm

"All researchers agree that the most difficult task in the Mie calculations is to find the partial wave coefficients." (Wang and van de Hulst, Appl. Opt., 1991). These authors have provided an algorithm, based on the ratio method, which they used in rainbow computations for *millimeter*-sized droplets. As has been seen, the a_{np} involve extensive computations of Riccati-Bessel, -Neuman, and -Hankel functions along with their derivatives. These functions satisfy the relations

$$F_{n-1}(z) + F_{n+1}(z) = (2n+1)F_n(z)/z \tag{75}$$

$$F_n'(z) = -nF_n(z)/z + F_{n-1}(z). \tag{76}$$

The first of these relations allows one to express the ratio ψ_n/ψ_{n-1} as a downward recurrence formula:

$$p_n(z) = \frac{\psi_n}{\psi_{n-1}} = \frac{1}{(2n+1)/z - p_{n+1}(z)}. \tag{77}$$

Denoting the Riccati-Neumann functions as χ_n, Eq.(75) also provides the forward recurrence

$$q_n(x) = \frac{\chi_n}{\chi_{n-1}} = \frac{2n-1}{x} - \frac{1}{q_{n-1}(x)}. \tag{78}$$

One may now write the ratios F_n'/F_n in terms of p_n or q_n:

$$\mathcal{A}_n(z) = \frac{\psi_n'}{\psi_n} = -n/z + 1/p_n(z) \tag{79}$$

and

$$\mathcal{B}_n(x) = \frac{\chi_n'}{\chi_n} = -n/x + 1/q_n(x). \tag{80}$$

In terms of these newly introduced quantities, the Lorenz-Mie coefficients may be written as

$$a_{n1} = \left[1 + i\frac{\chi_n(\varrho)}{\psi_n(\varrho)}\frac{\mathcal{A}_n(\eta) - \mathsf{m}\mathcal{B}_n(\varrho)}{\mathcal{A}_n(\eta) - \mathsf{m}\mathcal{A}_n(\varrho)}\right]^{-1} \tag{81}$$

and

$$a_{n2} = \left[1 + i\frac{\chi_n(\varrho)}{\psi_n(\varrho)}\frac{\mathsf{m}\mathcal{A}_n(\eta) - \mathcal{B}_n(\varrho)}{\mathsf{m}\mathcal{A}_n(\eta) - \mathcal{A}_n(\varrho)}\right]^{-1}. \tag{82}$$

One obtains $\psi_n(\varrho)$ and $\chi_n(\varrho)$ simply, from

$$\psi_n(\varrho) = \psi_1(\varrho)\prod_{i=2}^{n} p_i(\varrho) \tag{83}$$

and

$$\chi_n(\varrho) = \chi_1(\varrho) \prod_{i=2}^{n} q_i(\varrho), \tag{84}$$

with $\psi_1(\varrho) = \sin\varrho/\varrho - \cos\varrho$ and $\chi_1(\varrho) = \cos\varrho/\varrho + \sin\varrho$.

When the Wronskian relation for $\psi_n(\varrho)$ and $\chi_n(\varrho)$ can be used, the partial wave coefficients can be written as

$$a_{n1} = \left[1 + i\frac{\chi_n(\varrho)}{\psi_n(\varrho)}\left(1 - \frac{\mathsf{m}}{\chi_n^2(\varrho)\, r_n(\varrho)\,[\mathcal{A}_n(\eta) - \mathsf{m}\mathcal{A}_n(\varrho)]}\right)\right]^{-1} \tag{85}$$

and

$$a_{n2} = \left[1 + i\frac{\chi_n(\varrho)}{\psi_n(\varrho)}\left(1 - \frac{1}{\chi_n^2(\varrho)\, r_n(\varrho)\,[\mathsf{m}\mathcal{A}_n(\eta) - \mathcal{A}_n(\varrho)]}\right)\right]^{-1}. \tag{86}$$

It is generally found that χ_n is stable with respect to forward recursion and that $r_n(\eta_1) \to 0, |\eta_1| \ll n$.

In the implementation of these relations in FULMIE, the quantities

$$r_n(\varrho) = \frac{\psi_n(\varrho)}{\chi_n(\varrho)} \tag{87}$$

$$\varpi_1 = \psi_n(\varrho)\chi_n(\varrho) = \chi_n^2(\varrho)\, r_n(\varrho) \tag{88}$$

$$Y_1 = \mathcal{A}_n(\eta) - \mathsf{m}\mathcal{A}_n(\varrho) \tag{89}$$

$$Y_2 = \mathsf{m}\mathcal{A}_n(\eta) - \mathcal{A}_n(\varrho) \tag{90}$$

have been introduced. These allow one to write the partial wave coefficients as

$$a_{n1} = \left[1 + \frac{i}{r_n(\varrho)}\left(1 - \frac{\mathsf{m}}{\varpi_1 Y_1}\right)\right]^{-1} \tag{91}$$

and

$$a_{n2} = \left[1 + \frac{i}{r_n(\varrho)}\left(1 - \frac{1}{\varpi_1 Y_2}\right)\right]^{-1}, \tag{92}$$

and this eliminates the need to calculate $\mathcal{B}_n(\varrho)$ and q_n, and the $p_n(\varrho), p_n(\eta)$ are found from upward, downward recurrence, respectively.

It has been observed that $\langle\cos(\vartheta)\rangle$ ceases to change beyond $\eta \approx 1000$, however, when running the code for very large spheres (size parameters larger than about 40,000) the expansion in Eqn. 27 was found to break away abruptly from its converged value and tend toward 0.

5.1.2 The Q_{abs} algorithm

There are circumstances where one may wish to calculate Q_{abs} as a direct expansion rather than as a difference $(Q_{ext} - Q_{sca})$. One instance where this has been helpful is in the study of MDR effects on Q_{abs} in weakly absorbing droplets and droplet pairs. Another reason is that it can provide an additional internal check of the overall calculation. In the event that $\Im(\eta)$ becomes sufficiently large, $\psi'_n(\eta)$ and $\psi^*_n(\eta)$ will produce overflow errors (which is the major reason for utilizing the log-derivative, ratio algorithms in the first place).

From Eqns. (26 and 79), and the expression for C_{abs} [Eqn. (24)], we write Q_{abs} as

$$Q_{abs} = \frac{2}{\varrho^2}\sum_{n=1}^{\infty}\frac{(2n+1)}{|\psi_n(\varrho)|^2}\Re\left[i\mathcal{A}_n(\eta)\left(\mathsf{m}\left|\frac{a_{n1}}{Y_1}\right|^2 + \mathsf{m}^*\left|\frac{a_{n2}}{Y_2}\right|^2\right)\right], \tag{93}$$

thus avoiding, at least for uncoated spheres, the need to calculate $\psi_n(\eta)$ and ${\psi'}_n(\eta)$.

5.1.3 The τ_{mnp} algorithm

As a preparation for breaking out of the simplifying assumptions one encounters when dealing exclusively with plane waves incident on spherical particles, the structure of the τ_{mnp} code retains the azimuthal index, though only the case $m = 1$ need be considered for practical applications.

The derivation of the recursions for the angle dependent functions is straightforward. Assuming that $m \geq 0$ for the time being, begin with the definition

$$\tau_{mn2}(x) = \frac{m}{\sqrt{1-x^2}}P_n^m(x), \tag{94}$$

and the equation

$$P_{n+1}^m(x) = \frac{2n+1}{n-m+1}xP_n^m(x) - \frac{n+m}{n-m+1}P_{n-1}^m(x). \tag{95}$$

One is then led to

$$\tau_{mn2} = \frac{2n-1}{n-m}x\tau_{m,n-1,2} - \frac{n+m-1}{n-m}\tau_{m,n-2,2} \qquad \text{when} \quad m < n. \tag{96}$$

If $m = n$ then the relation

$$P_{n+1}^{m+1}(x) = \sqrt{1-x^2}\,(2n+1)P_n^m(x) - P_{n-1}^{m+1}(x) \tag{97}$$

is used to show that

$$\tau_{n,n,2} = \frac{n(2n-1)}{n-1}\sqrt{1-x^2}\tau_{n-1,n-1,2}. \tag{98}$$

Now,

$$-\sqrt{1-x^2}\frac{d}{dx}P_n^m(x) = \frac{1}{2}\big[(n-m-1)(n+m)P_n^{m-1}(x) - P_n^{m+1}(x)\big]. \tag{99}$$

From this and the definition

$$\tau_{mn1}(x) = \sqrt{1-x^2}\frac{d}{d\,x}P_n^m(x) \tag{100}$$

it can be shown that

$$\tau_{mn1} = \frac{n+m}{m}\tau_{m,n-1,2} - \frac{n\,x}{m}\tau_{mn2}, \qquad m \neq 0, \tag{101}$$

where use has also been made of the expressions

$$\sqrt{1-x^2}\;P_n^{m+1}(x) = 2mxP_n^m(x) - (n+m)(n-m+1)\sqrt{1-x^2}\;P_n^{m-1}(x) \tag{102}$$

and

$$(n-m+1)\sqrt{1-x^2}\;P_n^{m-1}(x) = xP_n^m(x) - \;P_{n-1}^m(x). \tag{103}$$

When $m = 0$ the use of

$$\frac{d}{dx}P_n(x) = \frac{2n-1}{n-1}x\frac{d}{dx}P_{n-1}(x) - \frac{n}{n-1}\frac{d}{dx}P_{n-2}(x) \tag{104}$$

leads to

$$\tau_{0n1} = \frac{2n-1}{n-1}x\tau_{0,n-1,1} - \frac{n}{n-1}\tau_{0,n-2,1}. \tag{105}$$

The above relations are implemented through the starting values

$$\begin{array}{lll} \tau_{0,0,2} = 0 & \tau_{0,1,2} = 0 & \tau_{1,1,2} = 1 \\ \tau_{0,0,1} = 0 & \tau_{0,1,1} = \sqrt{1-x^2} & \tau_{1,1,1} = -x \end{array} \tag{106}$$

If $|\sin\vartheta| = 0$ then the τ_{mn2} are found as 0.5D0*DFLOAT(N*(N+1))*CN**(N-1) to avoid round-off error in the recursions. (This is not a major issue with $m = 1$, but as $m \to n$, it can be.)

5.2 FULKOT Routines

5.2.1 Calculation of the cap (ˆ) coefficients

First,

$$\begin{aligned} {}^1\hat{a}_{n1} &= \frac{\mathsf{m}_1\xi'_n(\rho_1)\xi_n(\eta_1) - \xi_n(\rho_1)\xi'_n(\eta_1)}{\mathsf{m}_1\xi'_n(\rho_1)\psi_n(\eta_1) - \xi_n(\rho_1)\psi'_n(\eta_1)} \\ &= -\frac{\xi_n(\eta_1)\xi_n(\rho_1)}{\psi_n(\eta_1)\xi_n(\rho_1)}\frac{\mathsf{m}_1\frac{\xi'_n(\rho_1)}{\xi_n(\rho_1)} - \frac{\xi'_n(\eta_1)}{\xi_n(\eta_1)}}{\mathsf{m}_1\frac{\xi'_n(\rho_1)}{\xi_n(\rho_1)} - \frac{\psi'_n(\eta_1)}{\psi_n(\eta_1)}} \end{aligned} \tag{107}$$

and

$$\begin{aligned} {}^1\hat{a}_{n2} &= \frac{\mathsf{m}_1\xi_n(\rho_1)\xi'_n(\eta_1) - \xi'_n(\rho_1)\xi_n(\eta_1)}{\mathsf{m}_1\xi_n(\rho_1)\psi'_n(\eta_1) - \xi'_n(\rho_1)\psi_n(\eta_1)}. \\ &= \frac{\xi_n(\eta_1)\xi_n(\rho_1)}{\psi_n(\eta_1)\xi_n(\rho_1)}\frac{\mathsf{m}_1\frac{\xi'_n(\eta_1)}{\xi_n(\eta_1)} - \frac{\xi'_n(\rho_1)}{\xi_n(\rho_1)}}{\mathsf{m}_1\frac{\psi'_n(\eta_1)}{\psi_n(\eta_1)} - \frac{\xi'_n(\rho_1)}{\xi_n(\rho_1)}} \end{aligned} \tag{108}$$

Recurrence relations of the form

$$p_n(\eta) = \frac{\psi_n(\eta)}{\psi_{n-1}(\eta)} = \frac{1}{(2n+1)/\eta - p_{n+1}(\eta)} \tag{109}$$

and

$$\hat{q}_n(\rho) = \frac{\xi_n(\rho)}{\xi_{n-1}(\rho)} = \frac{2n-1}{\rho} - \frac{1}{\hat{q}_{n-1}(\rho)}. \tag{110}$$

and ratios of the form

$$\mathcal{A}_n(\eta) = \frac{\psi'_n(\eta)}{\psi_n(\eta)} = -n/\eta + 1/p_n(\eta) \tag{111}$$

and

$$\mathcal{C}_n(\rho) = \frac{\xi'_n(\rho)}{\xi_n(\rho)} = -n/\rho + 1/\hat{q}_n(\rho) \tag{112}$$

are already at our disposal. and we write

$${}^1\hat{a}_{n1} = -\frac{\xi_n(\eta_1)}{\psi_n(\eta_1)}\frac{\mathsf{m}_1\mathcal{C}_n(\rho) - \frac{\xi'_n(\eta_1)}{\xi_n(\eta_1)}}{\mathsf{m}_1\mathcal{C}_n(\rho) - \mathcal{A}_n(\eta)} \tag{113}$$

and

$$ {}^1\hat{a}_{n2} = \frac{\xi_n(\eta_1)}{\psi_n(\eta_1)} \frac{\mathsf{m}_1 \frac{\xi'_n(\eta_1)}{\xi_n(\eta_1)} - \mathcal{C}_n(\rho)}{\mathsf{m}_1 \mathcal{A}_n(\eta) - \mathcal{C}_n(\rho)}. \tag{114} $$

We now introduce the expressions

$$ \hat{p}_n(\eta) = \frac{\xi_n(\eta)}{\xi_{n-1}(\eta)} = \frac{1}{(2n+1)/\eta - \hat{p}_{n+1}(\eta)} \tag{115} $$

and

$$ \mathcal{C}_n(\eta) = \frac{\xi'_n(\eta)}{\xi_n(\eta)} = -n/\eta + 1/\hat{p}_n(\eta) \tag{116} $$

and write

$$ {}^1\hat{a}_{n1} = -\frac{\psi_n(\eta_1) + i\chi_n(\eta_1)}{\psi_n(\eta_1)} \frac{\mathsf{m}_1 \mathcal{C}_n(\rho) - \frac{\xi'_n(\eta_1)}{\xi_n(\eta_1)}}{\mathsf{m}_1 \mathcal{C}_n(\rho) - \mathcal{A}_n(\eta)} \tag{117} $$

$$ = -\left[1 + i\frac{\chi_n(\eta_1)}{\psi_n(\eta_1)}\right] \frac{\mathsf{m}_1 \mathcal{C}_n(\rho) - \mathcal{C}_n(\eta)}{\mathsf{m}_1 \mathcal{C}_n(\rho) - \mathcal{A}_n(\eta)} \tag{118} $$

and

$$ {}^1\hat{a}_{n2} = \left[1 + i\frac{\chi_n(\eta_1)}{\psi_n(\eta_1)}\right] \frac{\mathsf{m}_1 \mathcal{C}_n(\eta) - \mathcal{C}_n(\rho)}{\mathsf{m}_1 \mathcal{A}_n(\eta) - \mathcal{C}_n(\rho)}. \tag{119} $$

Letting

$$ \hat{r}_n(\eta) = \frac{\psi_n(\eta)}{\chi_n(\eta)} \tag{120} $$

we may write

$$ \hat{p}_n(\eta) = \frac{\chi_n(\eta)\,(i + \hat{r}_n(\eta))}{\chi_{n-1}(\eta)\,(i + \hat{r}_{n-1}(\eta))} = \frac{(i + \hat{r}_n(\eta))}{(i + \hat{r}_{n-1}(\eta))} q_n(\eta). \tag{121} $$

Since

$$ \psi_n(\eta) = \psi_1(\eta) \prod_{i=2}^{n} p_i(\eta) \tag{122} $$

and

$$ \chi_n(\eta) = \chi_1(\eta) \prod_{i=2}^{n} q_i(\eta), \tag{123} $$

$$ \hat{r}_n(\eta) = \frac{\psi_1(\eta)}{\chi_1(\eta)} \frac{\prod_{i=2}^{n} p_i(\eta)}{\prod_{i=2}^{n} q_i(\eta)} = \frac{\psi_1(\eta)}{\chi_1(\eta)} \prod_{i=2}^{n} \frac{p_i(\eta)}{q_i(\eta)} = \prod_{i=1}^{n} \frac{p_i(\eta)}{q_i(\eta)}. \tag{124} $$

We may now express $\mathcal{C}_n(\eta)$ as

$$ \mathcal{C}_n(\eta) = -n/\eta + \frac{i + \hat{r}_{n-1}(\eta)}{i + \hat{r}_n(\eta)} \frac{1}{q_n(\eta)}. \tag{125} $$

and ${}^1\hat{a}_{n1}$ and ${}^1\hat{a}_{n2}$ as

$$ {}^1\hat{a}_{n1} = -\left[1 + \frac{i}{\hat{r}_n(\eta)}\right] \frac{\mathsf{m}_1 \mathcal{C}_n(\rho) - \mathcal{C}_n(\eta)}{\mathsf{m}_1 \mathcal{C}_n(\rho) - \mathcal{A}_n(\eta)} \tag{126} $$

$$ = -\frac{1}{\hat{r}_n(\eta)} \left[i + \hat{r}_n(\eta)\right] \frac{\mathsf{m}_1 \left[-n/\rho + 1/\hat{q}_n(\rho)\right] - \left[-n/\eta + \frac{(i+\hat{r}_{n-1}(\eta))}{(i+\hat{r}_n(\eta))} 1/q_n(\eta)\right]}{\mathsf{m}_1 \left[-n/\rho + 1/\hat{q}_n(\rho)\right] - \left[-n/\eta + 1/p_n(\eta)\right]} \tag{127} $$

and

$$ {}^1\hat{a}_{n2} = \left[1 + \frac{i}{\hat{r}_n(\eta)}\right] \frac{\mathsf{m}_1 \mathcal{C}_n(\eta) - \mathcal{C}_n(\rho)}{\mathsf{m}_1 \mathcal{A}_n(\eta) - \mathcal{C}_n(\rho)} \tag{128} $$

$$ = \frac{1}{\hat{r}_n(\eta)} \left[i + \hat{r}_n(\eta)\right] \frac{\mathsf{m}_1 \left[-n/\eta + \frac{(i+\hat{r}_{n-1}(\eta))}{(i+\hat{r}_n(\eta))} 1/q_n(\eta)\right] - \left[-n/\rho + 1/\hat{q}_n(\rho)\right]}{\mathsf{m}_1 \left[-n/\eta + 1/p_n(\eta)\right] - \left[-n/\rho + 1/\hat{q}_n(\rho)\right]} \tag{129} $$

5.2.2 Calculation of the amplitude coefficients of the core

Let the index of refraction for the mantle be denoted m_1 with m_2 for the core and its size parameter ρ_2. Defining

$$\eta_+ = \rho_2\,\mathsf{m}_1 \tag{130}$$

$$\eta_- = \rho_2\,\mathsf{m}_2, \tag{131}$$

the reflection coefficients for the partial waves at the surface of the core can be expressed as

$${}^2a_{n1} = -\frac{\mathsf{m}\psi_n'(\eta_+)\,\psi_n(\eta_-) - \psi_n(\eta_+)\,\psi_n'(\eta_-)}{\mathsf{m}\xi_n'(\eta_+)\,\psi_n(\eta_-) - \xi_n(\eta_+)\,\psi_n'(\eta_-)} \tag{132}$$

and

$${}^2a_{n2} = -\frac{\mathsf{m}\psi_n(\eta_+)\,\psi_n'(\eta_-) - \psi_n'(\eta_+)\,\psi_n(\eta_-)}{\mathsf{m}\xi_n(\eta_+)\,\psi_n'(\eta_-) - \xi_n'(\eta_+)\,\psi_n(\eta_-)}, \tag{133}$$

where $\mathsf{m} = \mathsf{m}_2/\mathsf{m}_1$. Following the algorithm development for the coefficients of homogeneous spheres, we cast the coefficients of the core in the form

$${}^2a_{n1} = -\left[1 + i\frac{\chi_n(\eta_+)}{\psi_n(\eta_+)}\frac{\mathcal{A}_n(\eta_-) - \mathsf{m}\mathcal{B}_n(\eta_+)}{\mathcal{A}_n(\eta_-) - \mathsf{m}\mathcal{A}_n(\eta_+)}\right]^{-1} \tag{134}$$

and

$${}^2a_{n2} = -\left[1 + i\frac{\chi_n(\eta_+)}{\psi_n(\eta_+)}\frac{\mathsf{m}\mathcal{A}_n(\eta_-) - \mathcal{B}_n(\eta_+)}{\mathsf{m}\mathcal{A}_n(\eta_-) - \mathcal{A}_n(\eta_+)}\right]^{-1}, \tag{135}$$

or as

$${}^2a_{n1} = -\left[1 + \frac{i}{r_n(\eta_+)}\left(1 - \frac{\mathsf{m}}{\chi_n^2(\eta_+)\,r_n(\eta_+)\,[\mathcal{A}_n(\eta_-) - \mathsf{m}\mathcal{A}_n(\eta_+)]}\right)\right]^{-1} \tag{136}$$

and

$${}^2a_{n2} = -\left[1 + \frac{i}{r_n(\eta_+)}\left(1 - \frac{1}{\chi_n^2(\eta_+)\,r_n(\eta_+)\,[\mathsf{m}\mathcal{A}_n(\eta_-) - \mathcal{A}_n(\eta_+)]}\right)\right]^{-1}. \tag{137}$$

5.2.3 Calculation of Spherical Bessel Functions for Large $\Im(\eta)$

Note if $\psi_n = \exp w$, then $w = \log|\psi_n| + i\,Arg\,(\psi_n) + 2n\pi i$. It is assumed at this point that only the principal value need be of concern, and we define $w = \log\psi_n = \ln|\psi_n| + i\,Arg\,(\psi_n)$. To force the calulation when $\Im(\eta)$ exceeds 350, the code includes options that calculate

$$\begin{aligned}\psi_n'(\eta)\,\psi_n^*(\eta)\left(\mathsf{m}\,|c_{n1}|^2 + \mathsf{m}^*\,|c_{n2}|^2\right) &= \exp\left[\log\left(\psi_n'(\eta)\,\psi_n^*(\eta)\mathsf{m}\,|c_{n1}|^2\right)\right] \qquad (138)\\ &\quad + \exp\left[\log\left(\psi_n'(\eta)\,\psi_n^*(\eta)\mathsf{m}^*\,|c_{n2}|^2\right)\right]\\ &= \exp\left(\log\psi_n'(\eta) + \log\psi_n^*(\eta) + \log\mathsf{m} + 2\ln|c_{n1}|\right) \qquad (139)\\ &\quad + \exp\left(\log\psi_n'(\eta) + \log\psi_n^*(\eta) + \log\mathsf{m}^* + 2\ln|c_{n2}|\right).\end{aligned}$$

which succeeds because $|c_{np}| \to 0$ once n exceeds TRNCPT. Because

$$\psi_n(\eta) = \psi_1(\eta) \prod_{i=2}^{n} p_i(\eta) \tag{140}$$

and

$$A_n(\eta) = \frac{\psi_n'}{\psi_n} = \frac{-n}{\eta} + 1/p_n(\eta) \tag{141}$$

we can avoid evaluating $\ln|\psi_n^*(\eta)|$ and $\ln|\psi'^*_n(\eta)|$ by writing

$$\log \psi_n(\eta) = \log \psi_1(\eta) + \sum_{i=2}^{n} \log p_i(\eta) \tag{142}$$

and

$$\log \psi_n'(\eta) = \log\left[\psi_n(\eta) A_n(z)\right] = \log \psi_n(\eta) + \log\left[A_n(\eta)\right]. \tag{143}$$

Since the $p_i(\eta)$ here represent ratios of Riccati-Bessel functions of contiguous order, they, and consequently the $A_n(\eta)$, remain manageable. Expressing the c_{np} as

$$c_{np} = \frac{i\mathsf{m}}{Y_p} \frac{a_{np}}{\psi_n(\eta)\psi_n(\rho)}, \tag{144}$$

$$2\ln|c_{np}| = 2\left[\ln\left|\frac{\mathsf{m}}{Y_p}\right| + \Re\left(\log a_{np}\right) - \Re\left(\log \psi_n(\eta)\right) - \ln|\psi_n(\rho)|\right], \tag{145}$$

since

$$\begin{aligned} \log w^* &= \ln|w^*| + i\, Arg\left[w^*\right] && (146)\\ &= \ln|w| - i\, Arg\left[w\right] && (147)\\ &= \left[\log w\right]^*. && (148) \end{aligned}$$

This also gives

$$\begin{aligned} \psi_n'(\eta)\, \psi_n^*(\eta) \left(\mathsf{m}\left|c_{n1}\right|^2 + \mathsf{m}^*\left|c_{n2}\right|^2\right) &= \exp\left\{\log A_n(\eta) + 2\Re\left[\log \psi_n(\eta)\right] + \log \mathsf{m} + 2\ln|c_{n1}|\right\} + \\ &\quad \exp\left\{\log A_n(\eta) + 2\Re\left[\log \psi_n(\eta)\right] + \log \mathsf{m}^* + 2\ln|c_{n2}|\right\}. \end{aligned} \tag{149}$$

If $\Im(\eta) > 700$ the funtions cdsin(η) and cdcos(η) can produce overflow errors, and the starting value

$$\psi_1(\eta) = \frac{\sin\eta}{\eta} - \cos\eta \tag{150}$$

is replaced with the approximation

$$\psi_1(\eta) \longrightarrow -\exp\left[\Im(\eta)\right] \exp\left[-i\Re(\eta)\right] \left[\frac{i}{\eta} - 1\right], \tag{151}$$

which follows from expressing sin and cos in terms of sinh and cosh.

5.2.4 Asymptotes for Downward Recursion

$$\psi_n(z) = z j_n(z) = \sqrt{z\pi/2} J_{n+1/2}(z) \tag{152}$$

$$\chi_n(z) = z y_n(z) = \sqrt{z\pi/2} Y_{n+1/2}(z) \tag{153}$$

In the limit of large n

$$J_\nu(z) \sim \frac{1}{\sqrt{2\pi\nu}} \left(\frac{e\,z}{2\nu}\right)^\nu \tag{154}$$

$$Y_\nu(z) \sim -\sqrt{\frac{2}{\pi\nu}} \left(\frac{e\,z}{2\nu}\right)^{-\nu} \tag{155}$$

Then

$$\frac{\psi_n(z)}{\psi_{n-1}(z)} = \frac{\frac{1}{\sqrt{2\pi\nu}} \left(\frac{e\,z}{2\nu}\right)^\nu}{\frac{1}{\sqrt{2\pi(\nu-1)}} \left(\frac{e\,z}{2(\nu-1)}\right)^{\nu-1}} \tag{156}$$

$$= \sqrt{\frac{\nu-1}{\nu}} \left(\frac{e\,z}{2}\right) \frac{\left(\frac{1}{\nu}\right)^\nu}{\left(\frac{1}{(\nu-1)}\right)^{\nu-1}} \tag{157}$$

$$= \sqrt{\frac{\nu-1}{\nu}} \left(\frac{e\,z}{2}\right) \underbrace{\left(\frac{\nu-1}{\nu}\right)^\nu}_{\approx 1/e} \left(\frac{1}{\nu-1}\right) \tag{158}$$

$$= \frac{z}{2\sqrt{\nu\,(\nu-1)}} \tag{159}$$

Since $\sqrt{\nu\,(\nu-1)} \sim \nu - 1/2$ and $\nu = n + 1/2$ we arrive at

$$p_{N+1}(z) \to \frac{z}{2N+2}. \tag{160}$$

(If one had set $\nu - 1/2 \approx \nu$ then the starting value of $p_N(z) \to z/\,(2N+3)$ used van de Hulst is obtained.)

From a practical standpoint, as long as N is a few hundred more than the truncation index for the Mie series, the initial choice is pretty much irrelevant. The backward recursion for p_n rapidly 'gravitates' to the correct value. This seems to lead to a problem when one tries to construct q_n from by backward recursion: the p_n and q_n rapidly become one and the same, even though $q_{N+1} \approx 1/p_{N+1}$.

References

osajnl